



HAL
open science

1.7–18 μm mid-infrared supercontinuum generation in a dispersion-engineered step-index chalcogenide fiber

Arnaud Lemière, Rémi Bizot, Frédéric Désévéday, Grégory Gadret, Jean-Charles Jules, Pierre Mathey, Christophe Aquilina, Pierre Béjot, Franck Billard, Olivier Faucher, et al.

► To cite this version:

Arnaud Lemière, Rémi Bizot, Frédéric Désévéday, Grégory Gadret, Jean-Charles Jules, et al.. 1.7–18 μm mid-infrared supercontinuum generation in a dispersion-engineered step-index chalcogenide fiber. *Results in Physics*, 2021, 26, pp.104397. 10.1016/j.rinp.2021.104397 . hal-03437015

HAL Id: hal-03437015

<https://hal.science/hal-03437015>

Submitted on 19 Nov 2021

HAL is a multi-disciplinary open access archive for the deposit and dissemination of scientific research documents, whether they are published or not. The documents may come from teaching and research institutions in France or abroad, or from public or private research centers.

L'archive ouverte pluridisciplinaire **HAL**, est destinée au dépôt et à la diffusion de documents scientifiques de niveau recherche, publiés ou non, émanant des établissements d'enseignement et de recherche français ou étrangers, des laboratoires publics ou privés.

1.7-18 μm mid-infrared supercontinuum generation in a dispersion-engineered step-index chalcogenide fiber

Arnaud Lemière, Rémi Bizot, Frédéric Désévéday, Grégory Gadret, Jean-Charles Jules, Pierre Mathey, Christophe Aquilina, Pierre Béjot, Franck Billard, Olivier Faucher, Bertrand Kibler, * and Frédéric Smektala

Laboratoire Interdisciplinaire Carnot de Bourgogne (ICB), UMR6303 CNRS-Université Bourgogne Franche-Comté, 21000 Dijon, France

*Corresponding author: bertrand.kibler@u-bourgogne.fr

Abstract: We demonstrate 1.7-18 μm mid-infrared coherent supercontinuum generation by means of the full transmission window of a unique dispersion-engineered step-index Ge-Se-Te fiber. Our study thus opens the entire molecular fingerprint region to future chalcogenide fiber platforms.

Keywords: *optical fibers, supercontinuum, mid-infrared, chalcogenide glasses, nonlinear optics.*

Introduction: During the last decade there has been a surge of interest in developing mid-infrared (mid-IR) fiber-based supercontinuum (SC) sources [1-5]. Such broadband light sources take advantage of extreme spectral broadening of high-intensity laser pulses in infrared optical fibers usually made of soft glasses, such as chalcogenides that offer the widest transmission window and the highest nonlinearity [6]. Beyond their spatial coherence and high brightness, mid-IR fiber SC sources are nowadays operating over some wavelength ranges of thermal sources with superior performances for spectroscopic applications [7]. As an initial alternative to quantum cascade lasers, their capabilities are now compared to those of synchrotron IR beamlines for microscopy and spectroscopy [8]. Besides current challenges (replace bulky mid-IR pump lasers, simplify complex cascaded fiber systems and related fiber splicing, increase the power spectral density as well as keep an excellent pulse-to-pulse stability and a high degree of polarization),

research advances focused on extending the wavelength coverage over the entire mid-IR molecular fingerprint region (often defined as from 2 to 20 μm [9]) appear rather limited. In other words, intrinsic limitations of current fibers or even integrated waveguides now appear to impose the long-wavelength edge of mid-IR SC sources around 14-15 μm [1,3,10-12].

We here overcome this limitation by the engineered nonlinear transformation of femtosecond pulses over the full transmission window of a step-index chalcogenide fiber. In contrast to previous works, we reach the long-wavelength transparency edge of Se-rich glass family near 18 μm , and without including arsenic and antimony compounds considered as toxic elements and pollutants. Our end-to-end control of both material chemistry and nonlinear fiber optics, including glass synthesis and purification, fiber design and drawing, as well as engineering of SC generation, has allowed us to optimize each of these crucial steps in order to demonstrate coherent mid-IR SC generation spanning from 1.7 to 18 μm .

Results: The glass compositions here belong to the Ge-Se-Te ternary system for both core and cladding of our step-index fiber. More specifically, we have chosen the Se-rich part of the pseudo-binary $\text{GeSe}_4 - \text{GeTe}_4$, known to be compatible with fiber technology, from glass purification through distillation procedure to drawing operations [11,13]. The cladding and core compositions are $\text{Ge}_{20}\text{Se}_{70}\text{Te}_{10}$ and $\text{Ge}_{20}\text{Se}_{60}\text{Te}_{20}$, respectively. Glass rods are synthesized by the melt quenching method. Stoichiometric quantities of high purity elements (5N) are inserted into silica ampoules, then evacuated for several hours and heated up to remove superficial oxides as well as free water adsorbed on surface. Next, the precursors are gathered in the same ampoule in which oxygen and hydrogen getters (Al and TeCl_4) are added for further purification. The batch is then heated to fusion and further quenched in the glassy state, before to be first distilled under a dynamic vacuum. Volatile impurities are evacuated and trapped. Then, the silica ampoule in which the distilled glass has condensed is sealed and placed in a two-zone furnace for a second static distillation to separate the remaining traces of refractory particles (C, Al_2O_3 , or SiO_2) responsible for optical scattering. Finally, the glass batch is inserted into a rocking furnace for the last refining process, next quenched and finally annealed at $T_g - 5^\circ\text{C}$ for 12 h. Figure 1a (left panel) shows a typical Ge-Se-Te glass rod fabricated.

The glass transmission is measured for both glass compositions on a 5 mm-thick bulk sample from 1.3 to 25 μm . Similar absorption values are obtained for large-core fiber samples over a limited range (2-

11 μm), thus allowing to reconstruct a full curve of fiber losses as depicted in Fig. 1b. Our purification process is found to significantly decrease extrinsic absorption bands (O- and H- bonds). The background losses between 2 and 11 μm are negligible (below 0.06 dB/cm), when considering next experiments on cm-long fiber segments. Except the absorption near 13 μm related to remaining Ge–O bond, our Ge-Se-Te fiber exhibits a clear transmission window from the near-IR to its intrinsic multi-phonon absorption edge near 18 μm . The wavelength-dependent refractive indices for both glasses were calculated based on the Clausius–Mossoti relation and refractive index measurements [11,13]. The index difference is found to be about 0.09 over the mid-IR range. High numerical aperture ($\text{NA} > 0.6$) and a strong confinement of the fundamental guided mode are obtained with a simple step-index design (see Fig. 1a, center and right panels). Step-index preforms were fabricated by means of the rod-in-tube method, thus providing a suitable preform to draw step-index fibers with controllable outer and core diameters. For outer diameters in the 100–350 μm range, our core diameter can be selected from 6 to 20 μm (see example shown in Fig. 1a, right panel). By numerically solving the eigenvalue equation for cylindrical step-index waveguides, we found that a variety of dispersive properties can be explored in our step-index fibers, e.g., all-normal dispersion or multiple zero-dispersion wavelengths (ZDWs) [13]. Hence distinct nonlinear propagation regimes can be then explored to optimize SC generation [13–14]. For SC generation, we make use of a 12- μm -core diameter design (see Fig. 1a, right panel) which exhibits a rather flat dispersion curve associated with multi-ZDW features (see Fig. 1b), known to favor phase-matched frequency conversion over large bandwidths. Therefore, an input ultrashort pulse in the central anomalous dispersion region can provide strong energy transfer across both ZDWs (below 5.7 μm and beyond 12.6 μm) through efficient dispersive wave generation.

The experimental set-up used for SC generation is shown in Fig. 1c. High-power mid-IR femtosecond pulses, with tunable central wavelengths, are delivered by a non-collinear optical parametric amplifier (NOPA) followed by a difference-frequency generation (DFG) module. The NOPA is pumped by a chirped pulse amplified (CPA) Ti:sapphire system at 1 kHz repetition rate. Mid-IR pulses delivered by the DFG module exhibit μJ -level energy and temporal duration about 65 fs. The output laser beam is then focused on the chalcogenide fiber input facet with a ZnSe objective ($f = 6$ mm). The resulting SC light at the fiber output is collected with another ZnSe objective ($f = 12$ mm), and focused into a motorized monochromator with a gold-coated off-axis parabolic mirror. The monochromator includes two diffraction grating used for the 1.3–3 μm and 3–20 μm ranges. The output light is then sent onto a liquid nitrogen cooled HgCdTe

detector (with cutoff wavelength $\sim 22 \mu\text{m}$) by means of another gold-coated off-axis parabolic mirror. Several long-pass filters are inserted before the detector to avoid higher diffraction orders. The full SC is reconstructed by gathering the filtered spectra and adjusted by the system detection efficiency.

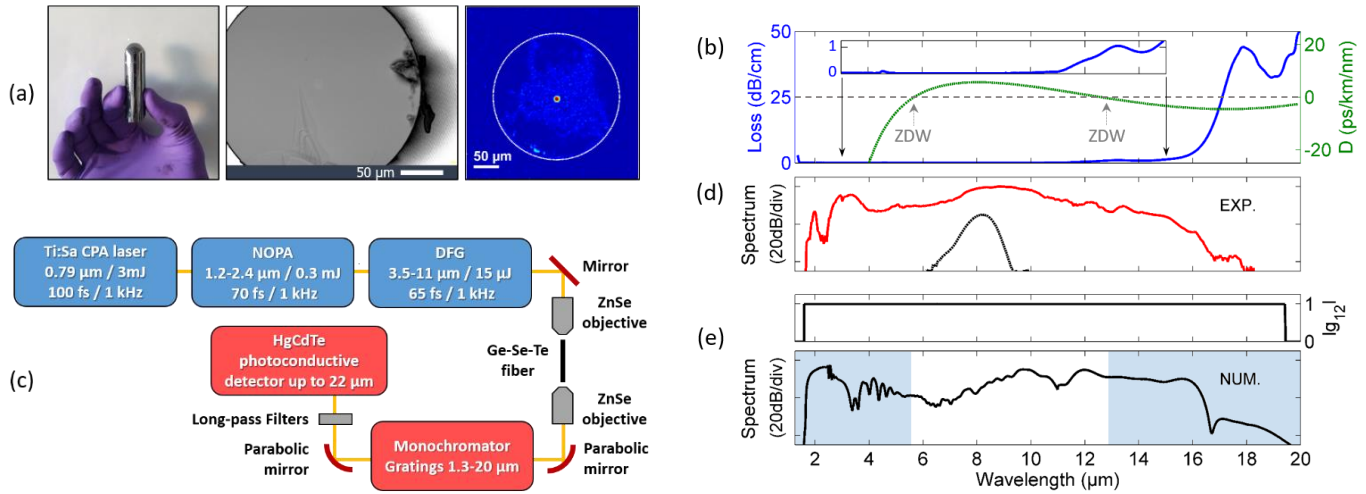


Figure 1. (a) From left to right: Synthesized Ge-Se-Te glass rod; Scanning electron microscope image of the cross-section of our 12- μm -core step-index fiber; Output near-field profile of the fundamental guided mode measured for an input broadband mid-IR source (the outer fiber diameter is indicated by the white circle). (b) Left axis, blue curve: Large-core fiber losses (inset: zoom on background losses). Right axis, green curve: Calculated dispersion profile D of fundamental guide mode for the 12- μm core Ge-Se-Te fiber. (c) Experimental setup for SC generation. (d) Measured output SC spectrum (red solid curve) from a 40-mm-long segment of 12- μm -core fiber. Input pulse spectrum centered at 8.15 μm (black dotted curve). (e) Corresponding numerical simulation (bottom panel: SC spectrum, top panel: first-order degree of coherence). Blue areas indicate regions with normal dispersion ($D < 0$).

Figure 1d shows the largest SC spectrum recorded, namely from 1.7 to 18 μm . This result was obtained when the input wavelength is centered at 8.15 μm and a coupled peak power about 200 kW **to avoid any damage issue (also related to low coupling efficiency)**. The fiber length was fixed to 40 mm, in order to provide enough propagation distance without detrimental impact of losses on SC extension as well practical manipulation of the fiber sample. We confirm spectral features of this broadband mid-IR SC through numerical simulations of the nonlinear pulse propagation in our fiber (based on the generalized nonlinear Schrödinger model), see Fig. 1e (bottom panel). This includes the full dispersion and loss curves, both Kerr and Raman nonlinear responses, and the dispersion of nonlinearity [11,14]. The spectral

broadening simply results from initial pulse compression with the anomalous dispersion and subsequent seeding of phase-matched dispersive waves in both regions of normal dispersion. Note that the energy transfer engineered across the particular second ZDW here overcomes potential issues of increasing absorption beyond 11 μm (related to different remaining impurities noticed in all the previous works [1,3,10-13]). The main limitations of SC extension on both wavelength edges now relate to the intrinsic optical bandgap ($\sim 1.5 \mu\text{m}$) and the multiphonon absorption ($\sim 18 \mu\text{m}$) of our Ge-Se-Te glass. The noise sensitivity of our SC source is also numerically characterized in Fig. 1e (top panel) through the complex degree of first-order coherence g_{12} over the full spectrum as described in Ref. [14]. A complete coherence is preserved over the SC spectrum in our engineered fiber, thus being of highly advantageous for practical applications.

Conclusion: In summary, we have taken a new step forward in the growing development of mid-IR fiber SC sources by overcoming demanding limitations at the interface between materials chemistry and nonlinear optics. More compact versions of similar SC sources are expected to be soon available by directly applying DFG to recent mid-IR femtosecond fiber lasers. Being close to cover the full molecular fingerprint region by means of a unique Ge-Se-Te fiber, the latter could be used as linear elements for highly sensitive evanescent optical sensing with engineered exposed lengths to the environment (D-shaped, side-polished, or ribbon fibers). All this offers a very promising route to successive key advances in mid-IR fiber-based technology and applications.

Acknowledgments. This work was supported by the Agence Nationale de la Recherche (EIPHI Graduate School, ANR-17-EURE-0002; PIA2/ISITE-BFC, ANR-15-IDEX-03), the European Regional Development Fund, and the Bourgogne-Franche-Comté Region.

Full References

- [1] C. R. Petersen, U. Møller, I. Kubat, B. Zhou, S. Dupont, J. Ramsay, T. Benson, S. Sujecki, N. Abdel-Moneim, Z. Tang, D. Furniss, A. Seddon, and O. Bang, "Mid-infrared supercontinuum covering the 1.4–13.3 μm molecular fingerprint region using ultra-high NA chalcogenide step-index fibre," *Nat. Photonics* **8**, 830 (2014).
- [2] Y. Yu, B. Zhang, X. Gai, C. Zhai, S. Qi, W. Guo, Z. Yang, R. Wang, D-Y. Choi, S. Madden, and B. Luther-Davies, "1.8–10 μm mid-infrared supercontinuum generated in a step-index chalcogenide fiber using low peak pump power," *Opt. Lett.* **40**, 1081 (2015)

- [3] Z. Zhao, B. Wu, X. Wang, Z. Pan, Z. Liu, P. Zhang, X. Shen, Q. Nie, S. Dai, and R. Wang, "Mid-infrared supercontinuum covering 2.0-16 μm in a low-loss telluride single-mode fiber," *Laser Photon. Rev.* **11**, 1700005 (2017).
- [4] S. Venck, F. St-Hilaire, L. Brilland, A. N. Ghosh, R. Chahal, C. Caillaud, M. Meneghetti, J. Troles, F. Joulain, S. Cozic, S. Poulain, G. Huss, M. Rochette, J. M. Dudley, and T. Sylvestre, "2-10 μm mid-infrared fiber-based supercontinuum laser source: Experiment and simulation," *Laser Photon. Rev.* **14**, 2000011 (2020).
- [5] R. A. Martinez, G. Plant, K. Guo, B. Janiszewski, M. J. Freeman, R. L. Maynard, M. N. Islam, F.L. Terry, O. Alvarez, F. Chenard, R. Bedford, R. Gibson, and A. I. Ifarraguerri, "Mid-infrared supercontinuum generation from 1.6 to $>11\mu\text{m}$ using concatenated step-index fluoride and chalcogenide fibers", *Opt. Lett.* **43**, 296 (2018).
- [6] G. Tao, H. Ebendorff-Heidepriem, A. M. Stolyarov, S. Danto, J. V. Badding, Y. Fink, J. Ballato, and A. F. Abouraddy, "Infrared fibers," *Adv. Opt. Photon.* **7**, 379 (2015).
- [7] I. Zorin, J. Kilgus, K. Duswald, B. Lendl, B. Heise, and M. Brandstetter, "Sensitivity-enhanced Fourier transform mid-infrared spectroscopy using a supercontinuum laser source," *Appl. Spectrosc.* **74**, 485 (2020).
- [8] C. R. Petersen, P. M. Moselund, L. Huot, L. Hooper, and O. Bang, "Towards a table-top synchrotron based on supercontinuum generation," *Infrared Phys. Technol.* **91**, 182 (2018).
- [9] N. Picqué and T. W. Hänsch, "Mid-IR spectroscopic sensing," *Opt. Photonics News* **30**, 26 (2019).
- [10] T. Cheng, K. Nagasaka, T. H. Tuan, X. Xue, M. Matsumoto, H. Tezuka, T. Suzuki, and Y. Ohishi, "Mid-infrared supercontinuum generation spanning 2.0 to 15.1 μm in a chalcogenide step-index fiber," *Opt. Lett.* **41**, 2117 (2016).
- [11] A. Lemièrre, F. Désévéday, B. Kibler, P. Mathey, G. Gadret, J-C. Jules, C. Aquilina, P. Béjot, F. Billard, O. Faucher and F. Smektala, "Mid-infrared two-octave spanning supercontinuum generation in a Ge–Se–Te glass suspended core fiber," *Laser Phys. Lett.* **16**, 075402 (2019).
- [12] M. Montesinos-Ballester, C. Lafforgue, J. Frigerio, A. Ballabio, V. Vakarin, Q. Liu, Joan M. Ramirez, X. Le Roux, D. Bouville, A. Barzaghi, C. Alonso-Ramos, L. Vivien, G. Isella, and D. Marris-Morini, "On-chip mid-infrared supercontinuum generation from 3 to 13 μm wavelength," *ACS Photon.* **7**, 3423 (2020).
- [13] A. Lemièrre, F. Désévéday, P. Mathey, P. Froidevaux, G. Gadret, J-C. Jules, C. Aquilina, B. Kibler, P. Béjot, F. Billard, O. Faucher and F. Smektala, "Mid-infrared supercontinuum generation from 2 to 14 μm in arsenic- and antimony-free chalcogenide glass fibers," *J. Opt. Soc. Am. B* **36**, A183 (2019).
- [14] G. Genty, S. Coen, and J.M. Dudley, "Fiber supercontinuum sources," *J. Opt. Soc. Am. B* **24**, 1771 (2007).